STEM CELLS®

REGENERATIVE MEDICINE

Electroacupuncture Promotes Central Nervous System-Dependent Release of Mesenchymal Stem Cells

TATIANA E. SALAZAR,[a,b,c] MATTHEW R. RICHARDSON,[d] ELENI BELI,[b] MATTHEW S. RIPSCH,[e,f] JOHN GEORGE,[c] YOUNGSOOK KIM,[e] YAQIAN DUAN,[b] LENI MOLDOVAN,[b] YUANQING YAN,[a] ASHAY BHATWADEKAR,[b] VAISHNAVI JADHAV,[e] JARED A. SMITH,[e] SUSAN MCGORRAY,[g] ALICIA L. BERTONE,[h] DMITRI O. TRAKTUEV,[i,j] KEITH L. MARCH,[i,j] LUIS M. COLON-PEREZ,[k] KEITH G. AVIN,[l] EMILY SIMS,[m] JULIE A. MUND,[d,m] JAMIE CASE,[m,n] XIAOLIN DENG,[o] MIN SU KIM,[p] BRUCE MCDAVITT,[q] MICHAEL E. BOULTON,[b] JEFFREY THINSCHMIDT,[r] SERGIO LI CALZI,[b] STEPHANIE D. FITZ,[s] ROBYN K. FUCHS,[l] STUART J. WARDEN,[l] TODD MCKINLEY,[t] ANANTHA SHEKHAR,[s] MARCELO FEBO,[k] PHILLIP L. JOHNSON,[u] LUNG-JI CHANG,[v,w] ZHANGUO GAO,[x] MIKHAIL G. KOLONIN,[x] SONG LAI,[y] JINGFENG MA,[y] XINZHONG DONG,[z] FLETCHER A. WHITE,[e,f] HUISHENG XIE,[aa] MERVIN C. YODER,[d,m] MARIA B. GRANT[b]

[a]Genetics Institute, [c]College of Medicine, [g]Department of Biostatistics, [k]Department of Psychiatry, McKnight Brain Institute, [r]Department of Pharmacology and Therapeutics, [w]Department of Molecular Genetics and Microbiology, [y]Department of Radiation Oncology, College of Medicine, [aa]College of Veterinary Medicine, University of Florida, Gainesville, Florida, USA, [b]Department of Ophthalmology, [d]Wells Center for Pediatric Research, [e]Department of Anesthesia, [s]Department of Psychiatry, [t]Department of Orthopedic Surgery, [u]Department of Anatomy and Cell Biology, Indiana University School of Medicine, Indianapolis, Indiana, USA, [f]Richard L. Roudebush VA Medical Center; [i]Krannert Institute of Cardiology, [j]Indiana Center for Vascular Biology and Medicine, [l]Department of Physical Therapy, School of Health and Rehabilitation Sciences, [m]Melvin and Bren Simon Cancer Center, Indiana University, Indianapolis, Indiana, USA; [h]Department of Veterinary Clinical Sciences, The Ohio State University, Columbus, Ohio, USA; [n]Scripps Clinic Medical Group, Scripps Center for Organ and Cell Transplantation, La Jolla, California, USA; [o]Mainland Acupuncture Center, Gainesville, Florida, USA; [p]College of Veterinary Medicine, Chon Buk National University, Jeonju, South Korea; [q]McDavitt Veterinary Clinic, Zionsville, Indiana, USA; [v]School of Medicine, University of Electronic Science and Technology of China, Sichuan, China; [x]The Brown Foundation, Institute of Molecular Medicine, University of Texas Health Science Center, Houston, Texas, USA; [z]Department of Neuroscience, Center of Sensory Biology, the Johns Hopkins University School of Medicine, Baltimore, Maryland, USA

Correspondence: Maria B. Grant, M.D., Department of Ophthalmology, Indiana University School of Medicine, 980 W. Walnut Street, R3-C426D, Indianapolis, Indiana 46202, USA. Telephone: +1-317-274-2628; Fax: 317-274-8046; e-mail: mabgrant@iupui.edu; or Mervin C. Yoder, M.D., Wells Center for Pediatric Research, Indiana University School of Medicine, 1044 West Walnut Street, R4-W125, Indianapolis, Indiana 46202, USA. Telephone: +1-317-274-4738; Fax: 317-274-8679; e-mail: myoder@iupui.edu

Received November 3, 2016; accepted for publication February 11, 2017; first published online in STEM CELLS *EXPRESS* March 16, 2017.

1066-5099/2017/$30.00/0

http://dx.doi.org/10.1002/stem.2613

The copyright line for this article was changed on 6 October 2017 after original online publication.

Key Words. Mesenchymal stem cells • Adult stem cells • Nervous system • Neurones

ABSTRACT

Electroacupuncture (EA) performed in rats and humans using limb acupuncture sites, LI-4 and LI-11, and GV-14 and GV-20 (humans) and *Bai-hui* (rats) increased functional connectivity between the anterior hypothalamus and the amygdala and mobilized mesenchymal stem cells (MSCs) into the systemic circulation. In human subjects, the source of the MSC was found to be primarily adipose tissue, whereas in rodents the tissue sources were considered more heterogeneous. Pharmacological disinhibition of rat hypothalamus enhanced sympathetic nervous system (SNS) activation and similarly resulted in a release of MSC into the circulation. EA-mediated SNS activation was further supported by browning of white adipose tissue in rats. EA treatment of rats undergoing partial rupture of the Achilles tendon resulted in reduced mechanical hyperalgesia, increased serum interleukin-10 levels and tendon remodeling, effects blocked in propranolol-treated rodents. To distinguish the afferent role of the peripheral nervous system, phosphoinositide-interacting regulator of transient receptor potential channels (Pirt)-GCaMP3 (genetically encoded calcium sensor) mice were treated with EA acupuncture points, ST-36 and LIV-3, and GV-14 and *Bai-hui* and resulted in a rapid activation of primary sensory neurons. EA activated sensory ganglia and SNS centers to mediate the release of MSC that can enhance tissue repair, increase anti-inflammatory cytokine production and provide pronounced analgesic relief. STEM CELLS *2017;35:1303–1315*

SIGNIFICANCE STATEMENT

In this study, we show how the use of electroacupuncture (EA) at specific points stimulates mesenchymal stem cell (MSC) release into peripheral blood through the activation of the nervous system. EA could be used to aid tissue repair through increasing the levels of circulating MSC. Moreover, MSC can be harvested directly from the blood of EA-treated humans and animals and expanded ex vivo. Thus, EA may be a low cost, low risk method for MSC harvest for autologous stem cell therapy.

INTRODUCTION

Acupuncture, one of the oldest medical therapies, mediates its therapeutic effect through the insertion of needles into specific points in the body called acupoints [1]. Electroacupuncture (EA) combines traditional acupuncture with modern electrotherapy as a means to enhance the stimulation at the acupoints. Acupoints are located in areas of decreased electrical resistance and increased electrical conductivity in the body attributed to both neural and vascular elements in the dermis or hypodermis [2]. Histological studies reveal that acupoints are located in areas with high densities of free nerve endings, arterioles, lymphatics, and mast cells

[3]. Certain acupoints have been identified to correspond to specific neural structures, such as superficial nerves and nerve plexuses [3].

The primary mechanism implicated in the anti-nociceptive effect of acupuncture involves release of opioid peptides in the central nervous system (CNS) in response to the long-lasting activation of ascending sensory tracks during the stimulation [1]. Adenosine has also been implicated, and interfering with adenosine metabolism prolonged the clinical benefit of acupuncture [4].

While both anatomical characteristics and local mediators of signaling are associated with specific acupoints, the mechanism responsible for the beneficial systemic effects and healing associated with acupuncture still lacks understanding. In this study, we sought to understand the central and peripheral nervous system response to EA using two sets of points (1: LI-4, LI-11, GV-14, *Bai-hui*; 2:ST-36, LIV-3, GV-14 and *Bai-hui*; Supporting Information Fig. S1) associated with successful treatment of arthritis and asthma and with modulation of immunity [5].

Results

EA Induces Activation of Hypothalamic Regions of the Brain in Both Rats and Humans

The systemic beneficial effects of EA may be centrally driven; therefore, we sought to determine the relationship between the hypothalamus and other brain structures, which is termed "connectivity." The hypothalamus plays a critical role as a primary homeostatic center in the brain and contains neurons with important projections to other limbic sites and sympathetic nuclei directly communicating with the periphery. To determine whether the hypothalamus was involved in the EA response, blood oxygen level-dependent (BOLD) functional magnetic resonance imaging (fMRI) was performed in anesthetized male Sprague-Dawley rats ($n = 6$) during a single EA session. Connectivity was derived from four time points: baseline, 0–8 minutes during EA, 9–22 minutes, and immediately post-EA. Seed regions included the anterior, posterior, and lateral hypothalamus. EA-stimulation produced changes in rats in the strength of functional connectivity within the hypothalamus and between the hypothalamus and adjacent brain regions, such as the amygdala (Fig. 1A), compared with baseline and the post-EA period. A representative example of the increase in signal (over time) in the PVN of a rat receiving acupuncture is shown in Figure 1B.

Arterial spin labeling fMRI was performed in healthy human subjects ($n = 6$) during a single EA session. Connectivity was derived from four time points: baseline, 0–8 minutes during EA, 8–16 minutes during EA, and immediately post-EA. EA stimulation produced changes in humans in the strength of functional connectivity within the hypothalamus and between the hypothalamus and adjacent brain regions (Fig. 2) compared with baseline and the post-EA period. Thus, rats and humans exhibited a similar response in terms of the connectivity observed.

As these regions have been associated with hematopoietic stem cell mobilization [6], peripheral blood was examined in the rat before and following EA for evidence of mesenchymal stem cell (MSC) mobilization. A 313% increase in the circulating MSC population, $Lin^-CD90^+CD44^{HI}$ cells, was detected in the blood of EA-treated rats 2 hours post-EA compared with baseline (Fig. 3A, 3B).

Characterization of Human EA Mobilized MSC as Adipocyte-Derived MSC

The availability of human antibodies to fully characterize the populations of cells mobilized by EA lead us to next examine the populations of cells mobilized by EA in the human subjects that underwent fMRI. Due to limitations regarding the fMRI equipment used, only points GV-14, LI-11, and LI-14 were able to be used in this experiment. We observed an increase in MSC in the peripheral blood 2 hours following EA in all subjects (Fig. 3C), while total lymphocyte numbers did not change. To further characterize the MSC population and potentially determine whether they were released from adipose stores, the levels of $CD34^+CD45^-CD31^-$ cells were examined. Two hours following completion of EA, $CD34^+CD45^-CD31^-$ cells were increased in four of six individuals (Fig. 3D) and the response was proportional to the body mass index of the subjects as previously noted [7]. Two individuals with body mass index less than 18.5 did not demonstrate an increase in this population. Human EA mobilized MSC were expanded in vitro and underwent adipogenic differentiation. Adipogenesis potential was confirmed by the cells' ability to form lipid droplets as established through oil red O staining (Fig. 3E–3H).

Because hypothalamic activation (Fig. 1B) preceded the mobilization of circulating MSC, it was proposed that the EA-induced connectivity changes contributed to the subsequent release of these cells into the peripheral blood. Exogenous administration of epinephrine or dopamine in rats resulted in a similar increase of $Lin^-CD90^{HI}CD44^+$ cell population into the circulation (Supporting Information Fig. S2A–S2C), supporting the role of CNS in mobilization of MSC and in EA activating these key CNS centers.

EA-Induced Uncoupling Protein 1 Expression Promotes the Browning of White Adipose Tissue in Rats

To confirm that EA can activate the sympathetic nervous system (SNS), we asked whether EA was associated with browning of white adipose tissue (WAT). The "inducible/recruitable" brown-like (beige a.k.a bright) adipocytes arise in WAT and are functionally indistinguishable from adipocytes in the canonical (constitutive) brown adipose tissue [8, 9]. The function of brown and beige adipocytes is muscle-independent thermogenic energy dissipation, which relies on the function of uncoupling protein 1 (UCP1) [10]. Following 14 days of EA (every other day) in rats, UCP1 immunofluorescence of inguinal subcutaneous WAT was increased (Fig. 4A), indicating a greater number of brown adipocytes, compared with control (sham EA) (Fig. 4B). Consistent with the notion that SNS signaling mainly activates subcutaneous WAT, no changes were detected in intraperitoneal WAT.

Pharmacological Disinhibition of the Dorsomedial Regions of the Tuberal Hypothalamus Mobilizes $Lin^-CD90^{HI}CD44^+$ Cells into the Circulation

To confirm that activation of the SNS can mediate release of MSC, we performed stereotaxic injections with the $GABA_A$ receptor antagonist bicuculline methiodide (BMI) in the

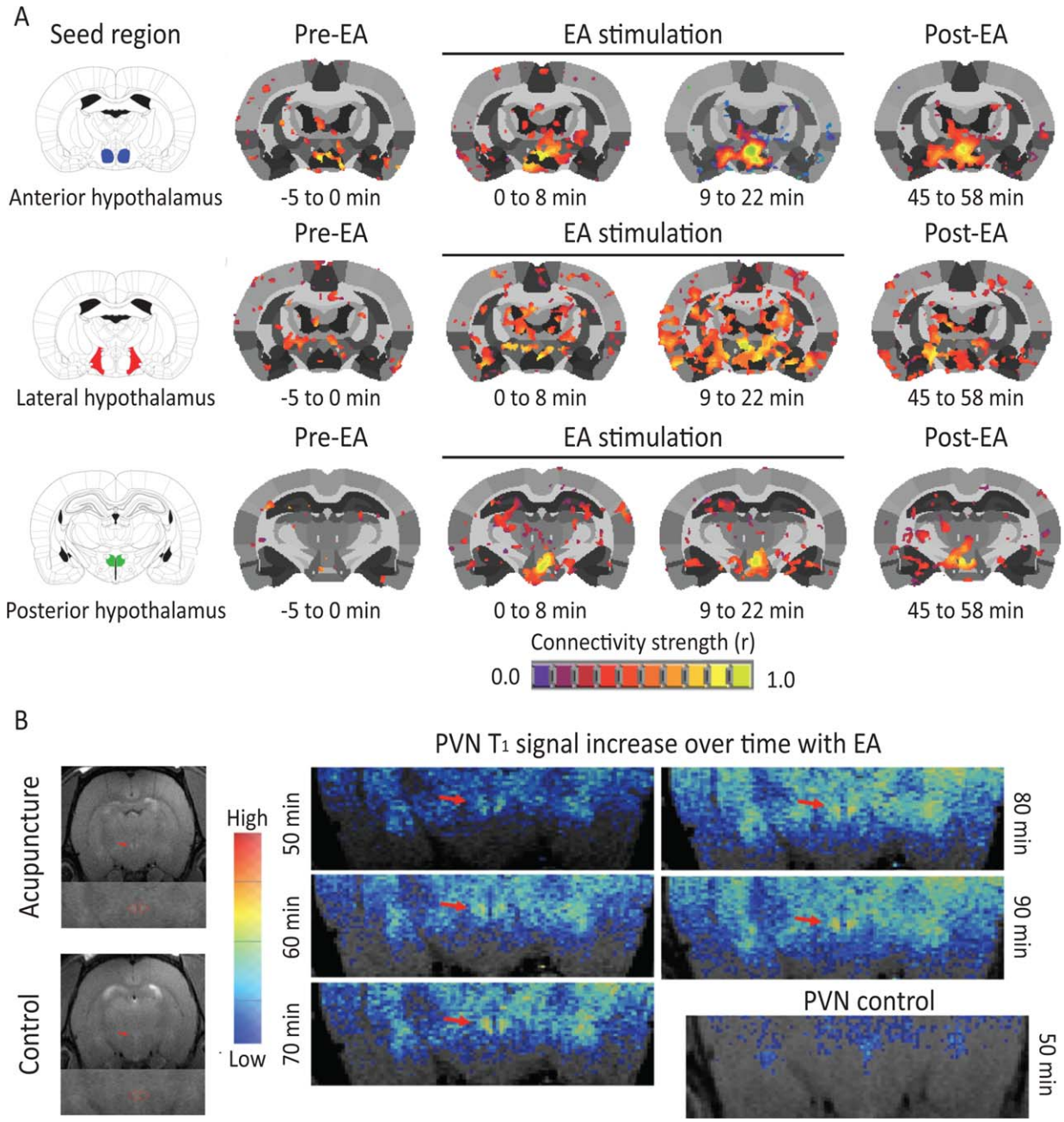

Figure 1. Electroacupuncture (EA) stimulation increases hypothalamic functional connectivity in rats. **(A)**: Rat brains were monitored through functional magnetic resonance imaging during administration of EA. Functional connectivity increased within the hypothalamus and between the hypothalamus and adjacent brain region with progression of treatment ($n = 6$). **(B)**: A representative example of the increase in signal (over time) in the PVN of a rat receiving acupuncture ($n = 1$). Abbreviations: EA, electroacupuncture; PVN, paraventricular nucleus.

dorsomedial regions of the tuberal hypothalamus to disinhibit these regions. Histological verification of injection sites is indicated in the illustration (Fig. 4C). The exact location of all injection sites are shown on coronal sections from a Standard Stereotaxic Atlas of the Rat Brain [11] (Fig. 4C) and a photomicrograph that shows the representative injection site (Fig. 4D). In rats, BMI at the dose of 50 pmol increased the percentage of circulating $Lin^-CD90^{HI}CD44^+$ cells ($F_{(2,\ 14)} = 6.7$, $p = .027$) at 4 hours post injection of BMI (Fig. 4E) in the absence of EA. These results demonstrate that circulating $Lin^-CD90^{HI}CD44^+$ cells are mobilized during hypothalamic disinhibition and EA. However, the delay in release (4 hours) compared with EA (2 hours) may suggest an alternative mechanism of release.

EA-Treated Rodents Exhibit Reduced Mechanical Hyperalgesia, Increased Serum Interleukin-10 Levels and Enhanced Tissue Remodeling following Partial Achilles Tendon Rupture

To address the possible anti-inflammatory and analgesic effects of EA-mobilization of circulating MSC [7], we analyzed the contribution of an EA treatment paradigm on injury-induced

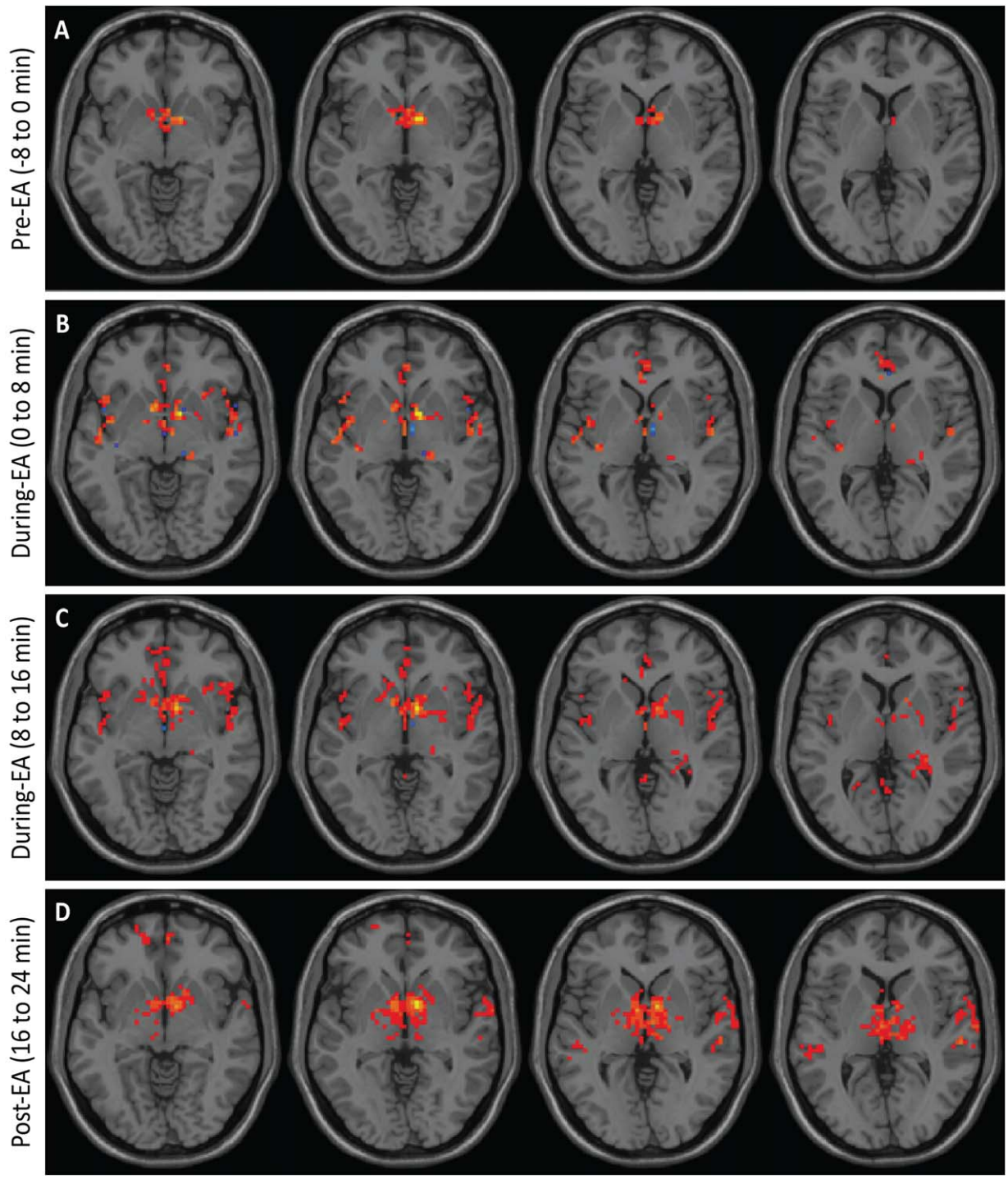

Figure 2. Electroacupuncture (EA) stimulation increases hypothalamic functional connectivity in humans. Brains from normal subjects were monitored using functional magnetic resonance imaging before, during, and after EA. Functional connectivity increased within the hypothalamus and between the hypothalamus and adjacent brain regions with progression of treatment ($n = 6$).

hyperalgesia in rats in the presence and absence of a β-blocker, propranolol. Treatments included EA (i.e., applied to the forelimb LI-4, LI-11, GV-14, and *Bai-hui*, and hindlimb ST36, LIV-3, GV-14 and *Bai-hui* immune points in horses), sham EA (i.e., applied to skin not associated with an acupoint) or EA plus propranolol (i.e., potential inhibitor for sympathetic effects of EA). EA or sham EA was administered every other day for 2 weeks following injury. Using sham EA applied to nonimmune acupoints or EA plus propranolol, nociceptive behavior elicited by von Frey mechanical stimulation did not change over the time course in the hind paw ipsilateral to the injury (Supporting Information Fig. S3). In contrast, mechanical hyperalgesia (assessed at both day 7 and 14) was considerably decreased (i.e., able to tolerate more pressure) in injured rodents subjected to EA application at LI-4, LI-11, GV-14, and *Bai-hui* (Fig. 5A). At early stages of tendon repair, the

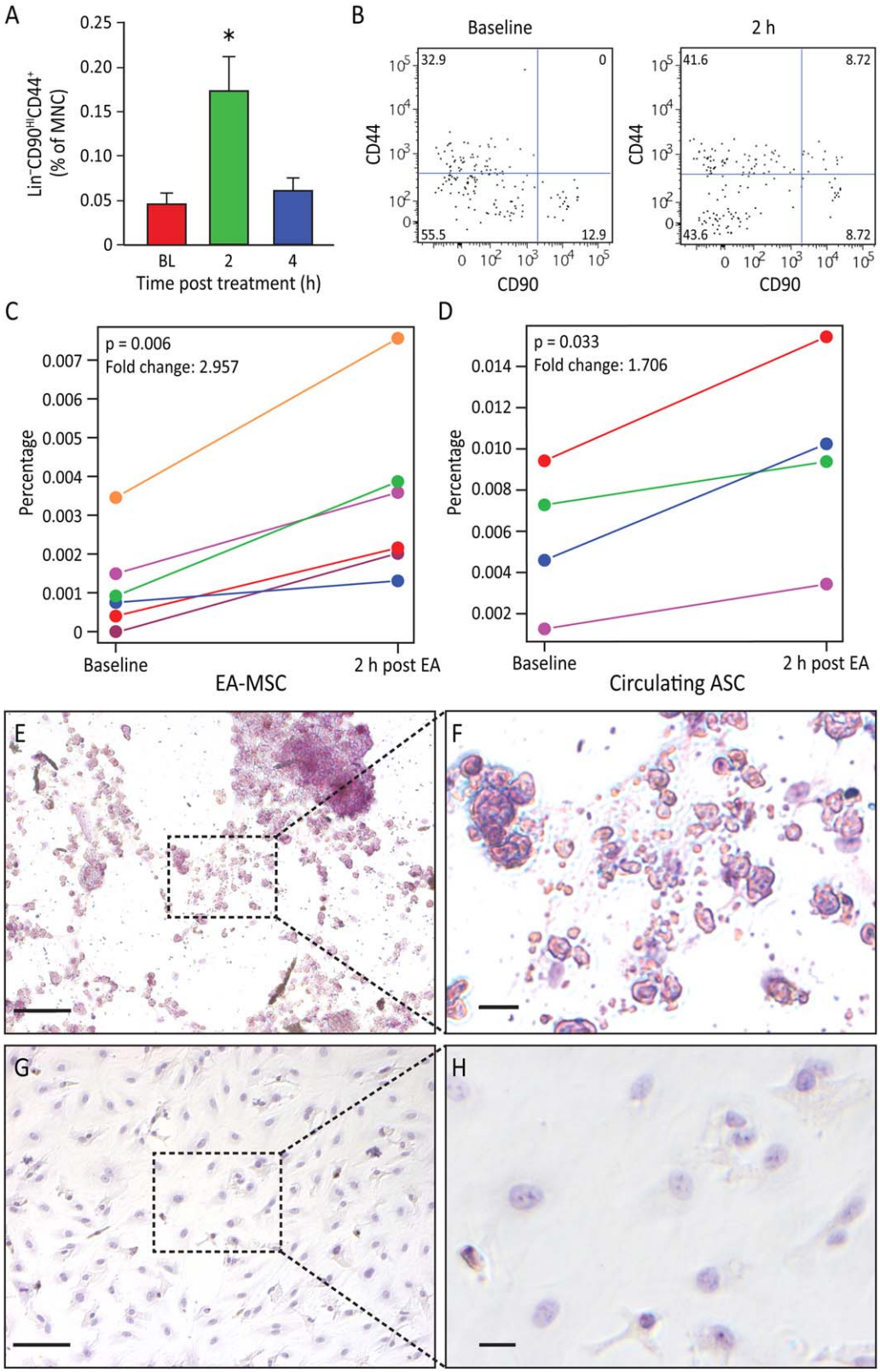

Figure 3. Electroacupuncture (EA) stimulation induced mesenchymal stem cell (MSC) mobilization. **(A)**: Rat peripheral blood MSC were increased ($p = .0063$) after EA. Circulating MSC were defined as Lin⁻(CD45⁻CD31⁻erythroid⁻CD11b⁻) cells that were positive for CD44 and CD90. Gated cells increased post treatment ($n = 11$ for baseline and 4 hours, $n = 9$ for 2 hours). **(B)**: Representative flow charts for rat Lin⁻ cells are shown at baseline and 2 hours samples. **(C)**: The percentage of human peripheral blood MSC increased in post EA-treatment ($p = .006$, $n = 6$). **(D)**: The percentage of circulating MSCs from adipose tissue (AD-MSC) is significantly elevated 2 hours post EA-treatment ($p = .033$, $n = 4$). **(E, F)**: EA-mobilized MSCs were expanded in vitro. After undergoing adipogenesis differentiation, EA-mobilized MSCs developed fat deposits as seen by Oil Red staining, which were not seen in the undifferentiated control cells **(G, H)**. Magnification bars = (E, G): 100 μm; (F, H): 50 μm. Abbreviations: ASC, adipose stem cells; EA, electroacupuncture; MNC, mononuclear cell.

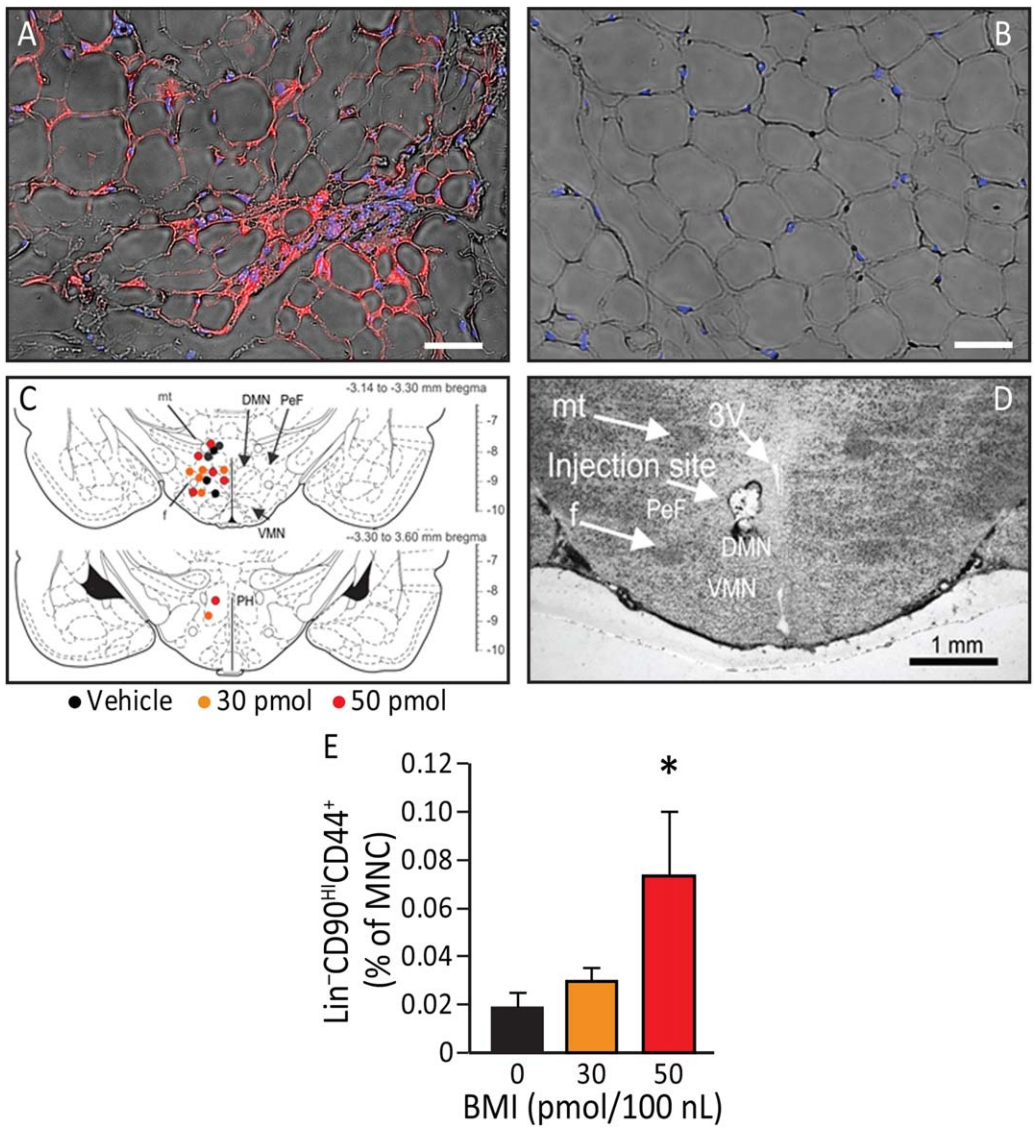

Figure 4. Electroacupuncture (EA) increases sympathetic activation leading to browning of white adipose tissue and the effects of EA can be duplicated by pharmacological disinhibition of hypothalamus (sympathetic activation). **(A, B)**: UCP1 immunofluorescence (red) detectable in inguinal subcutaneous adipose tissue (blue: adipocytes nuclei) from animals that underwent EA treatment (A) but not in control (B). EA resulted in an increase in beige adipocytes ($n = 4$). Magnification bars = 50 μm. **(C)**: The effects of EA can be duplicated by pharmacological disinhibition of hypothalamus. Rats underwent injection of either vehicle, 30 pmol or 50 pmol/100 nL of the $GABA_A$ receptor antagonist bicuculline methiodide. Sites of injections are represented on a coronal section from the tuberal hypothalamus from a Standard Steroetaxic Atlas of the Rat brain [11]. Colored circles indicate injection sites (black, orange, and red represent vehicle, 30 pmol and 50 pmol, respectively). **(D)**: Representative photomicrograph showing an injection site from one rat. Magnification bar = 1 mm. **(E)**: There was a significant increase ($p = .027$) in $Lin^-CD90^{HI}CD44^+$ cells in the plasma 4 hours post injection ($n = 6$). Data presented as means ± SEM. Abbreviations: BMI, bicuculline methiodide; DMN, dorsomedial hypothalamic nucleus; f, fornix; MNC, mononuclear cells; mt, mammillothalamic tract; PeF, perifornical hypothalamus; PH, posterior hypothalamic nucleus; VMN, ventromedial hypothalamic nucleus; 3V, third ventricle.

granulation tissues mainly synthesize type III collagen, while at later stages of healing, intrinsic fibroblasts produce type I collagen, whose fibers are orientated longitudinally to replace type III collagen. At 14 days post-injury, EA sham-treated or EA plus propranolol did not change type I collagen content, while type I collagen was significantly enhanced by EA (Fig. 5B); there was no change in type III collagen across treatments (Fig. 5C). Taken together, these data suggest that EA may enhance the replacement of thinner and immature type III collagen fibers with mature type I collagen fibers in the injured tendon [12], thereby supporting a better quality of regeneration and tissue reorganization. Given that EA can attenuate mechanical hyperalgesia and enhance tissue reorganization, we examined possible alterations of the anti-inflammatory cytokine, interleukin (IL)-10, in blood plasma. Previous evidence suggested that EA following surgical trauma contributed to increased levels of IL-10 by T-cells [13] and focal microinjections of IL-10 diminish mechanical hyperalgesia [14]. The results herein demonstrate that tendon injury in rodents subjected to sham EA or EA combined with propranolol fail to produce detectable changes in plasma IL-10. However, injured rodents treated with EA significantly increased IL-10 in plasma. These results indicate that EA

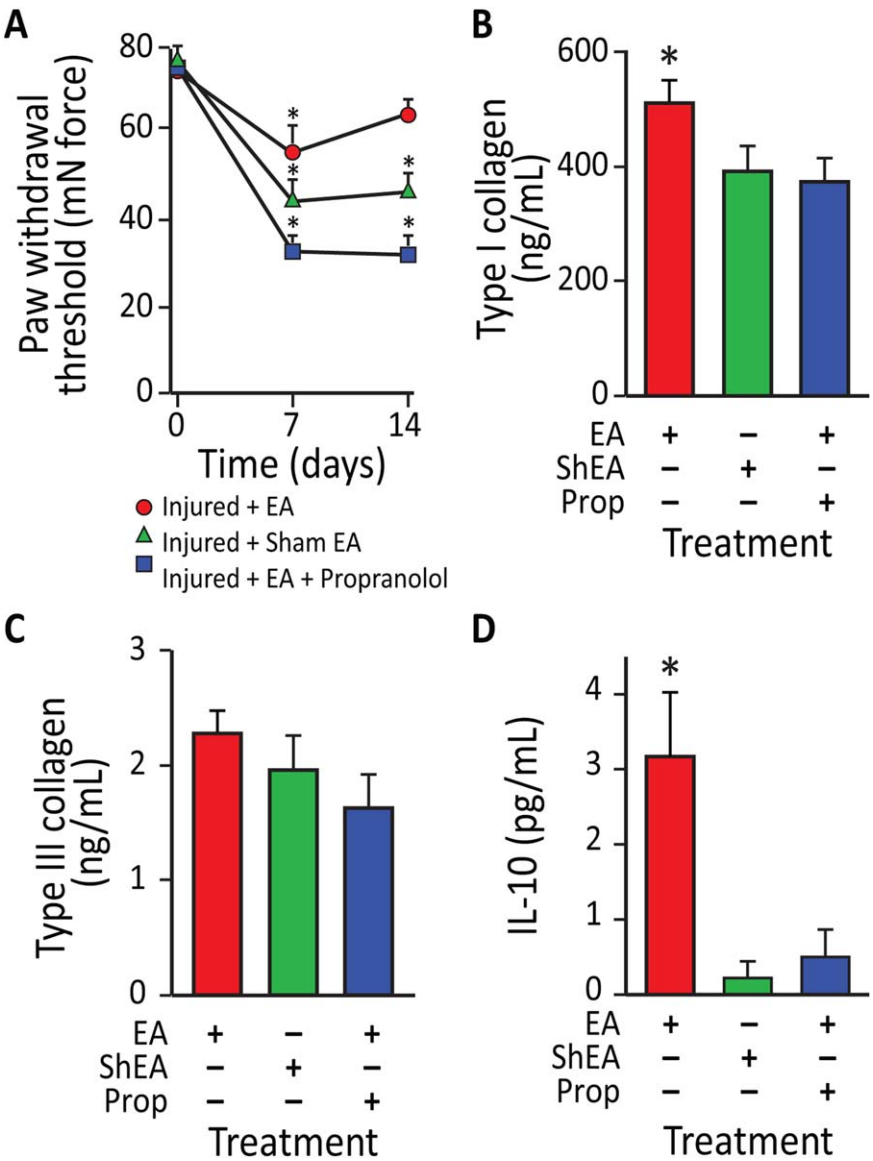

Figure 5. Electroacupuncture (EA)-treated rodents exhibit reduced mechanical hyperalgesia, enhanced tissue remodeling, and increased serum IL-10 levels following partial Achilles tendon rupture. **(A)**: Effects of EA application on mechanical allodynia in rats at 7 and 14 days after partial tendon rupture in the right hind leg. Mechanical hypersensitivity was determined by measuring the change in weight-bearing forces on the affected limb. Behavioral changes in the hind paw tactile threshold (in millinewtons, mN) were observed in the hindpaw ipsilateral to the tendon injury 18 hours after EA treatment, EA sham treatment or EA treatment with propranolol. (*, $p < .01$ versus baseline. EA: $n = 9$; EA: sham $n = 7$; EA + propranolol: $n = 10$). **(B)**: EA increased type I collagen content in injured tendons in rats at 14 days after unilateral Achilles tendon partial tenotomy. In EA-treated animals ($n = 6$), type-I collagen content was 24% greater in injured tendons than EA sham treated tendons ($n = 7$; $p < .05$) and 28% greater in injured tendons than EA + propranolol treated tendons ($n = 8$; $p < .02$). **(C)**: In contrast, there was no difference in type-III collagen content between injured EA and EA sham or EA + propranolol treated tendons ($p = .67$). **(D)**: IL-10 serum levels were also elevated in EA-treated rats compared with EA sham and EA + propanolol animals ($p = .0041$). Data presented as means ± SEM. Abbreviations: EA, electroacupuncture; IL-10, interleukin-10.

increases production of the endogenous anti-inflammatory cytokine IL-10 (Fig. 5D).

EA Performed over Immune Points in Pirt-GCaMP3 Mice Rapidly Activates Primary Sensory Neurons

We next examined mice to confirm that EA stimulation of acupoints (LI-4, LI-11, and GV-14 and *Bai-hui*) resulted in mobilization of MSC. At 4 hours post EA, murine MSC as defined by $Lin^-PDGFRa^+Sca\text{-}1^+$ cells were significantly increased ($p = .01$) in peripheral blood, a response that was markedly reduced when mice were pretreated with propranolol (Supporting Information Fig. S4). Immune acupoints are present on both the front and hind limbs of mice and are differentially used based on their ease of access in the particular species undergoing EA. Thus, we used acupoints in both front limbs (LI-4, LI-11) and hind limbs (ST-36 and LIV-3). To distinguish the afferent stimulation of the hypothalamus by peripheral acupoints, we treated Pirt-GCaMP3 mice with either a noxious hind paw pinch (100*g* force) or EA directed at the hind limb acupoints (Fig. 6A–6F) [15]. Hind paw stimulation evoked robust and transient Ca_2^+ increases in 10–20 neurons per DRG in naïve mice, on average 12.7 ± 3.0 per DRG (Fig. 6A, 6B) of which nearly all were small diameter neurons (<20 μm; Supporting Information Fig. S5;

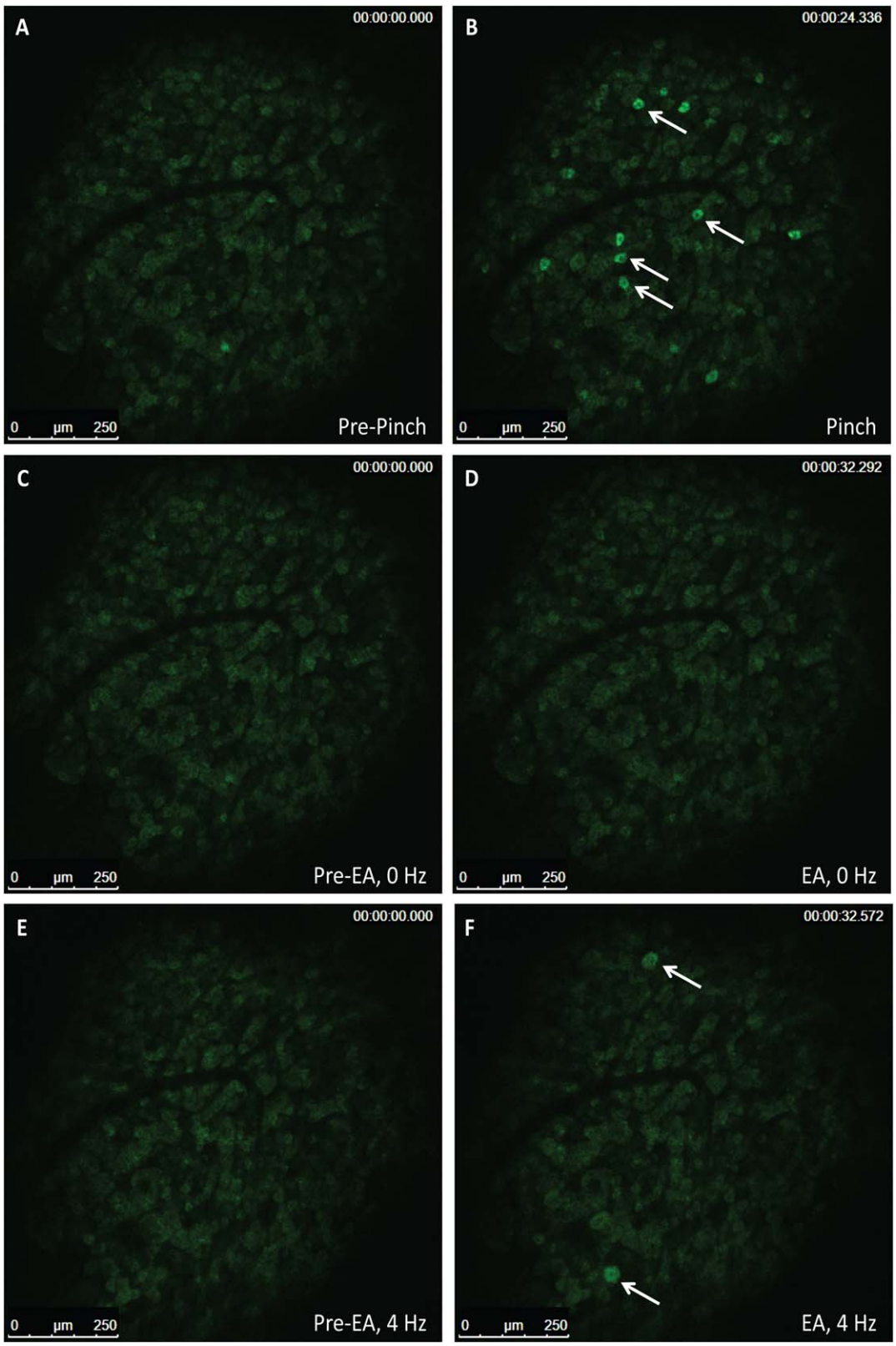

Figure 6. Small diameter primary afferent sensory neurons show sensitivity to pinch stimulus and medium-large diameter neurons show sensitivity to electroacupuncture (EA) in Pirt-GCaMP3 mice with intact dorsal root ganglia (DRG). Representative fluorescent GCaMP3 neuronal imaging response by lumbar DRG in vivo before **(A)** and after a mechanical press of the hindpaw using a 100*g* force **(B)**. The mechanical force evokes a robust fluorescent GCaMP3 Ca^{2+} response in numerous small sensory neurons (B; white arrows). Acupuncture needles alone failed to elicit neuronal changes in the same lumbar DRG of the Pirt-GCamp3 mouse **(C, D)**. EA-stimulation of the ST-36 and LIV-3 accupoints produced rapid activation of medium–larger diameter of the lumbar DRG (**E, F**; white arrows) ($n = 4$, $p < .0001$). Abbreviation: EA, electroacupuncture.

Supporting Information Video 1) suggestive of pain fibers. Placement of acupuncture needles alone did not elicit activity in sensory neurons (Fig. 6C, 6D; Supporting Information Video 2). We noticed a striking pattern of neuronal activation in the DRG following EA stimulation; many activated neurons were medium to large diameter neurons (medium [20–25 μm]; large [>25 μm] with an average of 6.1 ± 4.0 neurons per ganglia; (Fig. 6E, 6F; Supporting Information Video 3) suggesting activation of touch fibers.

EA at Immune Points in the Forelimbs Preferentially Mobilizes MSC Whereas EA of Immune Points in the Hind Limb Mobilizes Macrophages into the Circulation

Acupuncture of horses and humans is pursued with the same rigor and is not as technically difficult as acupuncture in rodents. We examined the forelimb (LI-4, LI-11, and GV-14 and *Bai-hui*) and hind limb immune points (ST36, LIV-3, and GV-14 and *Bai-hui*) in horses. Peripheral blood of horses ($n = 30$) undergoing EA at LI-4, LI-11, and GV-14 and *Bai-hui* was examined first. However, due to the limited availability of equine MSC antibodies compared with humans and mice, stem cell mobilization into peripheral blood was confirmed by measuring circulating cell colony-forming ability in vitro. While colony-forming cells were rarely seen at baseline, colony-forming ability was easily detected in blood samples obtained 2 and 4 hours after EA (Fig. 7A), the identical time points examined in humans and rats. Blood collected at 2 and 4 hours post-EA using mock acupoints approximately 1 cm from the immune points in the same horses did not give rise to colonies in vitro. Importantly, and representing a more critical control than simply sham acupoints, the use of metabolic points similarly did not give rise to significantly more colonies in vitro (Fig. 7A). To further verify the stem/progenitor characteristics of the equine cells, clonogenic potential was determined using single cell assays. EA-mobilized cells showed robust clonogenic potential, with over 75% proliferating into two or more cells, and over 50% of them resulting in large colonies of 10,000 cells or more; levels of proliferation that are generally reflective of stem/progenitor cells (Fig. 7B). The MSC origin of the mobilized colony forming cells was confirmed by their in vitro differentiation into osteocytes as demonstrated by positive staining for calcium deposits, (Fig. 7C, panels a, b [controls: panels e, f]), as well as their adipogenic differentiation (Fig. 7C, panels c, d [controls: panels g, h]) and chondrogenic differentiation (Fig. 7C, panels i, j) supporting that equine EA-mobilized cells display MSC lineage characteristics. When the EA-mobilized equine cells were examined in the in vivo angiogenesis assay, the cells did not directly form blood vessels (Fig. 7D, panel a) or lumenize; thus supporting a nonendothelial origin. However co-implantation of the EA-mobilized equine cells with human cord blood derived endothelial colony forming cells (ECFCs) significantly enhanced ECFC vasculogenesis (Fig. 7D, panels b, c) and the number of human vessels with an arterial morphology (Fig. 7E). Furthermore, when the EA-mobilized MSC were co-cultured with human ECFC (hECFC) in vitro, a significant increase in *HEY2* expression was observed in the endothelial cells, which indicated that the addition of the equine cells promoted arteriogenesis, as the Notch signaling pathway is known to be active in arterial vascular endothelial cells (Fig. 7F). Overall, these data support that EA-mobilized cells display MSC characteristics and enhance hECFC vasculogenesis and arteriogenesis.

To compare the EA-mobilized MSC (EA-MSC) with other MSC populations derived from either depots of adipose stem cells (ASC) or the bone marrow (BM-MSC), we performed gene array studies. Of the ~30,000 genes present on the EquGene-1_0-st GeneChip, 678 showed significant differences between EA-MSC and BM-MSC, 1,164 between the EA-MSC and ASC and 1,193 between ASC and BM-MSC (all $p < .05$ and absolute fold change >2) (Supporting Information Tables S1–S3). Principal component analysis mapping (Supporting Information Fig. S6A), hierarchical clustering (Supporting Information Fig. S6B), and partitioning clustering (Supporting Information Fig. S6C) showed that the EA-MSC, BM-MSC, and the ASC segregated into distinct groups. This suggests either that the EA-mobilized MSC population may be derived from a source distinct from either adipose tissue or bone marrow, or that their mobilization into the systemic circulation modified their gene expression from that of the BM-MSC or ASC obtained directly from their tissue source. Genes that were specifically upregulated in the EA-MSC cells compared with BM-MSC and ASC (Supporting Information Fig. S6C, Cluster 1) encoded numerous proteins with roles in cell cycle control and progression, DNA replication and repair, endothelial cell physiology, and adhesion and migration (*BGN*, *CTH*, DHFR, *ENG*, *EDN1*, *MYOF*, *PROCR*, *VEGF*, several integrins, and *SERPINB2*). In addition, this group contained genes coding for enzymes implicated in extracellular matrix synthesis, such as proteoglycans (e.g., *HAS2*, also possibly involved in vasculogenesis, *CHSY1*, *GCNT4*, etc.) and collagens (*COL1A1*, *COL1A2*, *COL3A1*, *COL5A1*, *COL5A2*, and *COL12A1*). Furthermore, EA-MSC cells expressed several growth hormones, hormone receptors, and members of their signaling pathways (*FGF5*, *BDNF*, *HTR2A*, *ADORA2B*, and *RLN*) (Supporting Information Tables S1 and S3).

Genes showing the greatest decreases in EA-MSC cells (Supporting Information Fig. S6C, Cluster 2) were acute-phase response genes and protease inhibitors (*HP*, *SAA1*, *JAM2*, *C1S*, *C1R*, and *SLPI*), concordant with the fact that stimulation of EA points reduces acute and chronic inflammation (Supporting Information Tables S2, S4).

The pathways in which were involved the genes differentially expressed between EA-MSC and BM-MSC were analyzed using Ingenuity Pathway Analysis software (IPA), and included cellular growth and proliferation, hepatic pathways and embryonic stem cell pluripotency, DNA damage response, axonal guidance signaling, cardiovascular system development, mitotic roles of polo-like kinase, as well as cell cycle: G2/M DNA damage checkpoint regulation, cell cycle control of chromosomal replication, GADD45 signaling, and ATM signaling (Supporting Information Table S5).

In contrast, BM-MSC demonstrated increased expression of genes involved in inflammatory responses (acute phase, cytokine signaling), cell motility, and response to hormones and growth factors (Supporting Information Fig. S6C, Cluster 3), while ASC displayed highly increased expression of genes related to cholesterol, fatty acids, and lipid metabolism, inflammatory response, and redox homeostasis (Supporting Information Fig. S6C, Cluster 4).

Changes in representative genes (*ADAM23*, *COL1A1*, *ENG*, *FGF5*, *GCNT4*, *HP*, *IGFBP3*, *RLN*, *SAA1* and *SERPINB2*) were further validated by real-time polymerase chain reaction (Supporting Information Fig. S7).

Contemporary interpretation of EA must consider contributions from the dry needle as well as the electrical stimulation itself, as performed in clinical applications such as

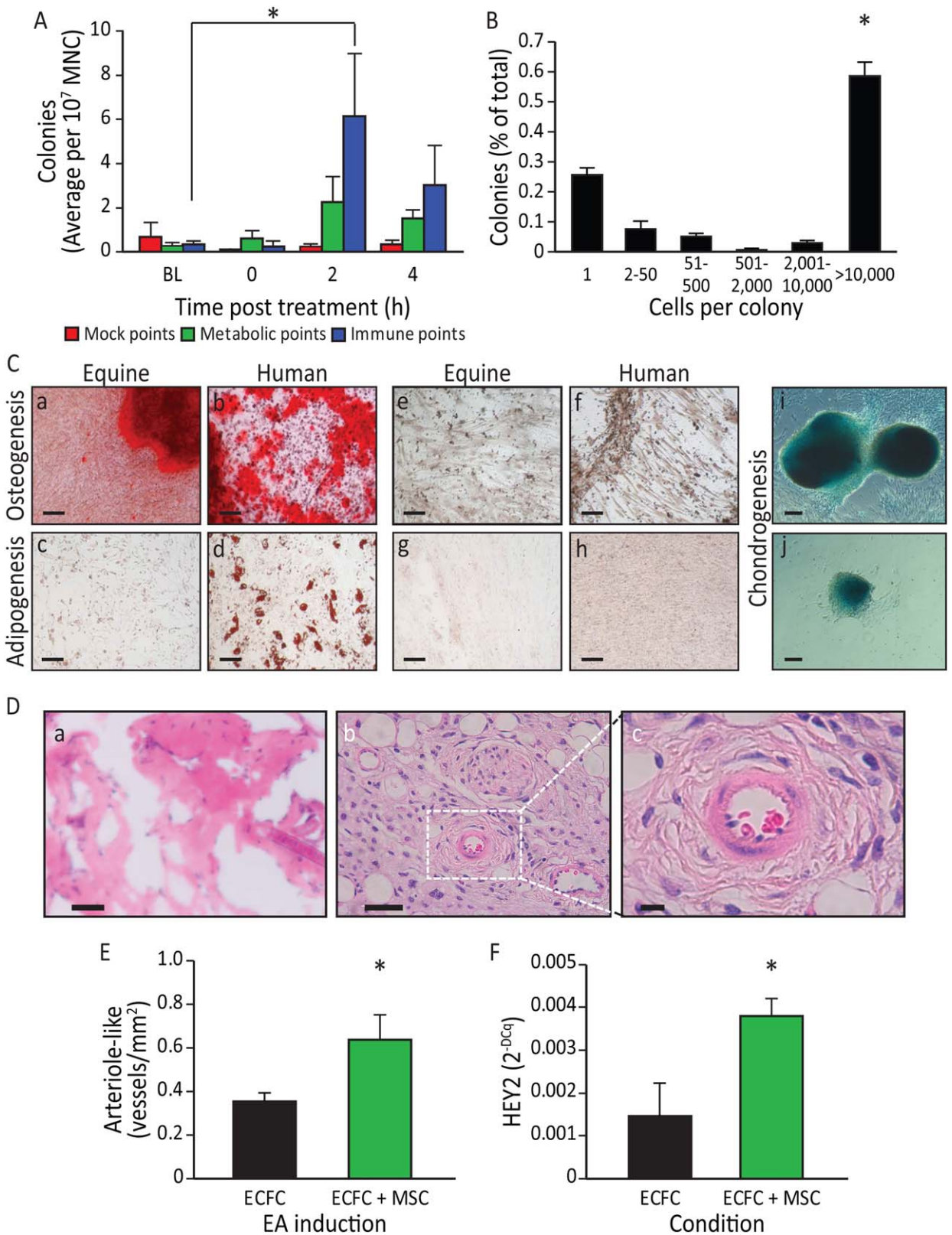

Figure 7.

transcutaneous electrical stimulation (TENS). Therefore, we next asked whether TENS performed with adhesive electrodes versus EA placed at immune acupoints LI-4, LI-11, and GV-14 and *Bai-hui* would result in similar MSC mobilization. All horses ($n = 6$) stimulated with TENS at LI-4, LI-11, and GV-14 and *Bai-hui* resulted in mobilization of MSC as confirmed by growth of MSC cultures (Supporting Information Fig. S8) from the 2 hours peripheral blood sample obtained following TENS.

As shown in Figure 6, EA at ST-36 and Liv-3 results in the activation of medium to large diameter neurons suggesting activation of touch fibers. EA at ST-36 and Liv-3 and GV-14 and GV-20 resulted in the release of cells exhibiting the appearance of macrophages, which was confirmed by their ability to phagocytose fluorescently-labeled *Escherichia coli* particles (Supporting Information Fig. S9).

Discussion

In this study, we make the highly novel observation that EA at immune points releases key populations in the peripheral blood (MSC and macrophages) that can modulate physiological responses to injury. While the effect of EA on analgesia is well-accepted, until now the effect of EA on release of reparative cell populations is largely unknown. Of equal importance is that the effect of EA we observed is uniform across four species. The fMRI studies in both humans and rats support that EA activates the hypothalamus leading to mobilization of MSC. These cells can be ex vivo expanded and they demonstrate the phenotypic and functional characteristics of MSC. Depending on the set of immune points used the reparative population released varies. When the EA at GV-14 and *Bai-hui* is performed with the forelimb points (LI-4 and LI-11), MSC are released into the blood, whereas when EA at GV-14 and *Bai-hui* is performed with the hind limb (ST-36 and LIV-3) points macrophage-like cells are released instead (Supporting Information Fig. S1). Similar responses to those observed with forelimb immune points were observed with injections of either epinephrine or dopamine and with pharmacological disinhibition of the tuberal hypothalamus with the $GABA_A$ receptor antagonist bicuculline methiodide in rats. Pharmacological disinhibition of the tuberal hypothalamus increases plasma concentration of norepinephrine by 100% and epinephrine by 400% [16]. Deep brain stimulation of the tuberal hypothalamus of humans also enhances sympatho-excitation [17]. Furthermore, these electrical activities could be replaced by TENS stimulation at the precise EA points. Thus, the mobilization of MSCs is likely centrally mediated through hypothalamic activation and subsequent SNS activity. There has been increasing interest and evidence supporting the role of the SNS as a regulator of immune cell release, as appropriate activation and signaling is necessary to mobilize these cells into the blood stream [6].

TENS is a widely accepted method of pain relief [18]. The use of TENS over acupoints is a relatively new application, with some using the term transcutaneous EA [19]. Methods to mobilize circulating MSC (i.e., epinephrine, dopamine, substance P, and GM-CSF) or hematopoietic stem cells (i.e., chemotherapy, growth factors, or AMD3100 [20–23]) into the bloodstream are plagued by adverse side effects; however, use of EA or TENS represents an easy and inexpensive approach to increasing MSC numbers in the peripheral blood to allow MSC harvest and ex vivo expansion.

EA has been reported to have long-lasting and powerful analgesic effects in models of both acute and chronic pain [24, 25]. Adrenergic receptors or GABAergic modulation through peripheral, spinal, and supraspinal mechanisms, as well as adenosine A1 receptors have been implicated as part of the underlying mechanisms of this effect [4, 26–28]. EA-induced mobilization of circulating MSC may have served to directly or indirectly modulate anti-inflammatory and immunomodulatory properties in vivo [29, 30], as we show by the increase in serum IL-10 levels and the observed reduced mechanical hyperalgesia. This would suggest that EA limits the production of nociceptive proinflammatory cytokines and serves to enhance tissue remodeling following tendon injury [31–33]. In contrast, chronic treatment with the non-selective β-adrenergic receptor antagonist, propranolol, effectively blocks EA's anti-inflammatory activity [34, 35]. Monocyte mobilization into peripheral blood can also be mediated by sympathetic signaling [36]. In our studies, the use of hind-limb points mobilized a cell type that acquired a macrophage-like phenotype in culture and that presented strong phagocytic activity in vitro. These activated cells could be playing a role in modulation of the cytokine milieu leading to

Figure 7. Electroacupuncture (EA)-mediated sympathetic stimulation induces mesenchymal stem cell (MSC) release into the circulation. **(A)**: EA mobilized cells are highly proliferative and potentiate vasculogenesis. Equine peripheral blood mononuclear cells (MNC) showed an increased colony-forming ability 2 hours ($p < .05$) post administration of EA at immune points ($n = 7$), while cells obtained from the same horses when they underwent mock treatment or treatment at metabolic points did not. **(B)**: The EA-mobilized cells demonstrated high proliferative capacity, when plated in a single-cell assay, with over 50% proliferating into large colonies ($p < .001$ vs. all groups). **(C)**: Equine peripheral blood MNCs were cultured to the third passage and then differentiated into key mesenchymal lineages. **(a)**: Following culture with osteogenic induction media, the mobilized equine cells showed strong osteogenic potency, demonstrated by Alizarin red staining of calcium deposits (red: Alizarin red). **(b)**: Human mesenchymal cells responded in a similar fashion when cultured under identical conditions. Equine cells when cultured under control media (1:1 Ham's F12 and low glucose Dulbecco's modified Eagle's medium, 15% fetal bovine serum) **(e)** and human cells under control conditions **(f)** did not show Alizarin red staining. **(c)**: The EA-mobilized equine cells showed a weak adipogenic response, demonstrated by oil red O staining of lipid deposits (red: oil red O) when cultured under adipogenic conditions; **(d)** human MSC showed a much stronger response than the equine cells when cultured under identical adipogenic conditions. Under control conditions, neither equine MSCs **(g)** or human MSCs **(h)** showed oil red O staining. **(i, j)** When cells were cultured under chondrogenesis differentiation media they were able to differentiate into chondrogenic lineages, demonstrated by Alcian Blue staining of proteoglycans in the cell masses. Magnification bars = 50 μm. **(D)**: In vivo angiogenesis assay. **(a)**: When equine cells were incorporated into a three-dimensional type I pig skin collagen plug and placed under the skin of NOD/SCID mice no capillaries were formed. **(b)**: Human endothelial colony forming cells (hECFC) were inserted into the porcine collagen plugs together with equine MSC, and implanted into the flank of NOD/SCID mice. **(c)**: A higher magnification of the boxed area in **(b)**, showing a bona fide blood vessel. Magnification bars = **(a, b)**: 50 μm; **(c)**: 10 μm. **(E)**: When quantified, the hECFC-MSC had a significant increase of arteriogenesis compared with hECFC alone ($p = .02$, $n = 5$ for ECFCs alone, $n = 7$ for combined hECFC-MSC group). **(F)**: After 48 hours in vitro, cells were isolated, total mRNA was extracted and *HEY2* expression levels were quantified by quantitative real-time polymerase chain reaction. *HEY2* was elevated in the mixed cell treatment when compared with ECFC alone ($p = .006$, $n = 4$). All data presented as means ± SEM. Abbreviations: EA, electroacupuncture; ECFC, endothelial colony forming cell; MNC, mononuclear cell; MSC, mesenchymal stem cell.

EA-mediated repair and analgesia (Supporting Information Fig. S10). The specificity of cell mobilization according to the points warrants further study.

The activation of the SNS with EA is further supported by our results demonstrating that EA at the specific points LI-11, LI-4, GV-14, and *Bai-hui* promoted browning of WAT in rats. Brown adipose tissue counter-acts WAT function [37, 38]. This effect was accomplished using an every other day EA protocol for 14 days. Shen et al. [39] used points typically associated with treatment of obesity (acupoints ST-36 and ST-44) six times per week for 5 weeks in DIO mice to accomplish this same effect. They did not observe weight loss or a decrease in appetite in the EA-treated mice; however, they did observe a reduction in the ratio of WAT weight/body weight suggesting that EA increased lipolysis in obese mice. WAT "browning" is driven by SNS stimuli, such as cold temperature, and signal transduction cascades triggered by catecholamines activating β3 adrenergic receptors [37, 40, 41]. $UCP1^{+}$ thermogenic brown-like (beige/bright) adipocytes within WAT [42, 43] activate energy expenditure and can counteract metabolic consequences of obesity [44, 45]. Even a mild reduction in lipid content in WAT associated with its browning activates energy expenditure and has positive metabolic benefits [46, 47]. Fat browning has been considered as a promising avenue in diabetes treatment [48].

Conclusion

Acupuncture is among the oldest healing practices in the world and is currently one of the most rapidly growing complementary therapies. Our studies provide strong support for the use of EA at specific immune points to stimulate MSC and macrophage release into peripheral blood through hypothalamic and SNS activation. EA may serve as a way to facilitate tissue repair following injury by supplying high levels of circulating MSC into the circulation and could be used to treat acute or chronic conditions associated with inflammation [49, 50]. Furthermore, fMRI and direct neurostimulation studies have confirmed SNS activation and the metabolically beneficial response of browning of WAT. The importance of adiposity is demonstrated in individuals with body mass index of >18.5. We observed an increase in the specific subset of MSC, the ASC population only in these individuals. Importantly, EA stimulated "browning" of WAT can enhance metabolism and influence glucose sensitivity. Furthermore, harvesting of MSC from the blood of EA-treated human subjects and ex vivo expansion is feasible and may serve as a practical method to harvest cells for autologous cell therapy, free of the risks and discomfort associated with current more invasive and toxic collection methods.

Acknowledgments

We thank the Angio BioCore at Indiana University School of Medicine for their work in the human studies, the Flow Cytometry Resource Facility at Indiana University Simon Cancer Center (partially funded by National Cancer Institute Grant P30. CA082709), the OSUCCC Microarray Shared Resource, where the equine GeneChips were processed, and Christopher Brown for his original illustration, the graphical abstract. This work was supported by NIH Grants R01EY012601-15, R01HL11070-03, R01DK090730-04, and R01EY007739-23 (to M.B.G.), U54 DK106846-01 and R01 HL109602 (to M.C.Y.), PR151924 (to M.E.B.), and DK100905, R01DK100905 and 101BX002209 (to F.A.W.), by the St. Vincent Foundation (to F.A.W.) and by the Cryptic Masons' Medical Research Foundation (to K.L.M. and D.T.).

Author Contributions

T.E.S. and M.R.R.: study design, acquisition of data, data analysis and interpretation, manuscript writing, final approval of manuscript; E.B. and J.C.: study design, acquisition of data, data analysis and interpretation, manuscript writing; M.S.R., Y.D., A.B., V.J., J.A.S., A.L.B., D.O.T., S.D. B.M.D., S.L.C., S.D.F., R.K.F., S.J.W., and T.M.K: acquisition of data; J.G.: study design, acquisition of data; Y.K., Y.Y., L.M.C.-P., E.S., J.A.M., and P.L.J.: acquisition of data, data analysis and interpretation; L.M. and K.A.: acquisition of data, data analysis and interpretation, manuscript writing; S.M.G.: data analysis and interpretation; K.L.M.: study design; M.S.K.: study design, acquisition of data, data analysis and interpretation; M.E.B.: manuscript writing; J.T.: data acquisition, data analysis and interpretation, manuscript writing; A.S.: data analysis and interpretation; M.F., M.G.K., and F.A.W.: study design, data acquisition, data analysis and interpretation, manuscript writing; L.J.C., S.L., and X.D.: study design, data acquisition, data analysis and interpretation; Z.G.: data acquisition; J.M.: data acquisition and analysis; H.X.: study design, data acquisition, manuscript writing; M.C.Y.: study design, data analysis and interpretation, manuscript writing, final approval of manuscript; M.B.G.: conception of ideas, study design, data acquisition, data analysis and interpretation, manuscript writing, final approval of manuscript. T.E.S and M.R.R are first authors who contributed equally to this article. F.A.W., H.X, M.C.Y. and M.B.G are senior authors who contributed equally to this article.

Accession Numbers

Microarray data have been deposited in GEO and given the accession number GSE53723.

Disclosure of Potential Conflicts of Interest

The authors indicate no potential conflicts of interest.

References

1 Zhao ZQ. Neural mechanism underlying acupuncture analgesia. Prog Neurobiol 2008; 85:355–375.

2 Urano K, Ogasawara S. A fundamental study on acupuncture points phenomena of dog body. Kitasato Arch Exp Med 1978;51:95–109.

3 Gunn CC, Ditchburn FG, King MH et al. Acupuncture loci: A proposal for their classification according to their relationship to known neural structures. Am J Chin Med (Gard City NY) 1976;4:183–195.

4 Goldman N, Chen M, Fujita T et al. Adenosine A1 receptors mediate local anti-nociceptive effects of acupuncture. Nat Neurosci 2010;13:883–888.

5 Kim SK, Bae H. Acupuncture and immune modulation. Auton Neurosci 2010;157:38–41.

6 Katayama Y, Battista M, Kao WM et al. Signals from the sympathetic nervous system regulate hematopoietic stem cell egress from bone marrow. Cell 2006;124: 407–421.

7 Gil-Ortega M, Garidou L, Barreau C et al. Native adipose stromal cells egress from adipose tissue in vivo: Evidence during lymph node activation. Stem Cells 2013;31: 1309–1320.

8 Shinoda K, Luijten IH, Hasegawa Y et al. Genetic and functional characterization of clonally derived adult human brown adipocytes. Nat Med 2015;21:389–394.

9 Cypess AM, Haft CR, Laughlin MR et al. Brown fat in humans: Consensus points and experimental guidelines. Cell Metab 2014;20:408–415.
10 Bartness TJ, Shrestha YB, Vaughan CH et al. Sensory and sympathetic nervous system control of white adipose tissue lipolysis. Mol Cell Endocrinol 2010;318:34–43.
11 Paxinos G, Watson C. The Rat Brain in Stereotaxic Coordinates. Academic Press, Amsterdam, 2007.
12 Liu X, Wu H, Byrne M et al. Type III collagen is crucial for collagen I fibrillogenesis and for normal cardiovascular development. Proc Natl Acad Sci U S A 1997;94:1852–1856.
13 Wang K, Wu H, Wang G et al. The effects of electroacupuncture on TH1/TH2 cytokine mRNA expression and mitogen-activated protein kinase signaling pathways in the splenic T cells of traumatized rats. Anesth Analg 2009;109:1666–1673.
14 Shimizu K, Guo W, Wang H et al. Differential involvement of trigeminal transition zone and laminated subnucleus caudalis in orofacial deep and cutaneous hyperalgesia: The effects of interleukin-10 and glial inhibitors. Mol Pain 2009;5:75.
15 Kim YS, Anderson M, Park K et al. Coupled Activation of Primary Sensory Neurons Contributes to Chronic Pain. Neuron. 2016;91:1085–1096.
16 Wible JH, Jr, DiMicco JA, Luft FC. Hypothalamic GABA and sympathetic regulation in spontaneously hypertensive rats. Hypertension 1989;14:623–628.
17 Wilent WB, Oh MY, Buetefisch CM et al. Induction of panic attack by stimulation of the ventromedial hypothalamus. J Neurosurg 2010;112:1295–1298.
18 Wall PD, Sweet WH. Temporary abolition of pain in man. Science 1967;155:108–109.
19 Song J, Yin J, Chen J. Needleless transcutaneous electroacupuncture improves rectal distension-induced impairment in intestinal motility and slow waves via vagal mechanisms in dogs. Int J Clin Exp Med 2015;8:4635–4646.
20 Kumar S, Ponnazhagan S. Mobilization of bone marrow mesenchymal stem cells in vivo augments bone healing in a mouse model of segmental bone defect. Bone 2012;50:1012–1018.
21 Kassis I, Zangi L, Rivkin R et al. Isolation of mesenchymal stem cells from G-CSF-mobilized human peripheral blood using fibrin microbeads. Bone Marrow Transplantation 2006;37:967–976.
22 Broxmeyer HE, Orschell CM, Clapp DW et al. Rapid mobilization of murine and human hematopoietic stem and progenitor cells with AMD3100, a CXCR4 antagonist. J Exp Med 2005;201:1307–1318.
23 Kawada H, Fujita J, Kinjo K et al. Nonhematopoietic mesenchymal stem cells can be mobilized and differentiate into cardiomyocytes after myocardial infarction. Blood 2004;104:3581–3587.
24 Zhang RX, Lao L, Wang X et al. Electroacupuncture attenuates inflammation in a rat model. J Altern Complement Med 2005;11:135–142.
25 Huang C, Hu ZP, Long H et al. Attenuation of mechanical but not thermal hyperalgesia by electroacupuncture with the involvement of opioids in rat model of chronic inflammatory pain. Brain Res Bull 2004;63:99–103.
26 Zhang Y, Zhang RX, Zhang M et al. Electroacupuncture inhibition of hyperalgesia in an inflammatory pain rat model: Involvement of distinct spinal serotonin and norepinephrine receptor subtypes. Br J Anaesth 2012;109:245–252.
27 Koo ST, Lim KS, Chung K et al. Electroacupuncture-induced analgesia in a rat model of ankle sprain pain is mediated by spinal alpha-adrenoceptors. Pain 2008;135:11–19.
28 Silva JR, Silva ML, Prado WA. Analgesia induced by 2- or 100-Hz electroacupuncture in the rat tail-flick test depends on the activation of different descending pain inhibitory mechanisms. J Pain 2011;12:51–60.
29 Newman RE, Yoo D, LeRoux MA et al. Treatment of inflammatory diseases with mesenchymal stem cells. Inflamm Allergy Drug Targets 2009;8:110–123.
30 Chamberlain G, Fox J, Ashton B et al. Concise review: Mesenchymal stem cells: Their phenotype, differentiation capacity, immunological features, and potential for homing. Stem Cells. 2007;25:2739–2749.
31 Torres-Rosas R, Yehia G, Pena G et al. Dopamine mediates vagal modulation of the immune system by electroacupuncture. Nat Med 2014;20:291–295.
32 Chen XM, Xu J, Song JG et al. Electroacupuncture inhibits excessive interferon-gamma evoked up-regulation of P2X4 receptor in spinal microglia in a CCI rat model for neuropathic pain. Br J Anaesth 2015;114:150–157.
33 Inoue M, Nakajima M, Oi Y et al. The effect of electroacupuncture on tendon repair in a rat Achilles tendon rupture model. Acupunct Med 2015;33:58–64.
34 Choi JW, Kang SY, Choi JG et al. Analgesic effect of electroacupuncture on paclitaxel-induced neuropathic pain via spinal opioidergic and adrenergic mechanisms in mice. Am J Chin Med 2015;43:57–70.
35 Kim HW, Kang SY, Yoon SY et al. Low-frequency electroacupuncture suppresses zymosan-induced peripheral inflammation via activation of sympathetic post-ganglionic neurons. Brain Res 2007;1148:69–75.
36 McKim DB, Patterson JM, Wohleb ES et al. Sympathetic release of splenic monocytes promotes recurring anxiety following repeated social defeat. Biol Psychiatry 2016;79:803–813.
37 Rosen ED, Spiegelman BM. What we talk about when we talk about fat. Cell 2014;156:20–44.
38 Nedergaard J, Cannon B. The browning of white adipose tissue: Some burning issues. Cell Metab 2014;20:396–407.
39 Shen W, Wang Y, Lu SF et al. Acupuncture promotes white adipose tissue browning by inducing UCP1 expression on DIO mice. BMC Complement Altern Med 2014;14:501.
40 Enerback S. The origins of brown adipose tissue. N Engl J Med 2009;360:2021–2023.
41 Cinti S. Transdifferentiation properties of adipocytes in the adipose organ. Am J Physiol Endocrinol Metab 2009;297:977–986.
42 Wu J, Bostrom P, Sparks LM et al. Beige adipocytes are a distinct type of thermogenic fat cell in mouse and human. Cell 2012;150:366–376.
43 van Marken Lichtenbelt WD, Vanhommerig JW, Smulders NM et al. Cold-activated brown adipose tissue in healthy men. N Engl J Med 2009;360:1500–1508.
44 Tseng YH, Cypess AM, Kahn CR. Cellular bioenergetics as a target for obesity therapy. Nat Rev Drug Discov 2010;9:465–482.
45 Lowell BB, S-Susulic V, Hamann A et al. Development of obesity in transgenic mice after genetic ablation of brown adipose tissue. Nature 1993;366:740–742.
46 Reilly SM, Chiang SH, Decker SJ et al. An inhibitor of the protein kinases TBK1 and IKK-varepsilon improves obesity-related metabolic dysfunctions in mice. Nat Med 2013;19:313–321.
47 Orci L, Cook WS, Ravazzola M et al. Rapid transformation of white adipocytes into fat-oxidizing machines. Proc Natl Acad Sci U S A 2004;101:2058–2063.
48 Yoneshiro T, Aita S, Matsushita M et al. Recruited brown adipose tissue as an anti-obesity agent in humans. J Clin Invest 2013;123:3404–3408.
49 Ringden O, Uzunel M, Rasmusson I et al. Mesenchymal stem cells for treatment of therapy-resistant graft-versus-host disease. Transplantation 2006;81:1390–1397.
50 Le Blanc K, Rasmusson I, Sundberg B et al. Treatment of severe acute graft-versus-host disease with third party haploidentical mesenchymal stem cells. Lancet 2004;363:1439–1441.

See www.StemCells.com for supporting information available online.